

# Dispersive Corrections to the Born Approximation in Elastic Electron-Nucleus Scattering in the Intermediate Energy Regime

P. Guèye,<sup>1</sup> A. A. Kabir,<sup>1,2</sup> J. Glistler,<sup>3,4,5</sup> B. W. Lee,<sup>6</sup> R. Gilman,<sup>7</sup> D. W. Higinbotham,<sup>8</sup> E. Piasetzky,<sup>9</sup> G. Ron,<sup>9</sup> A. J. Sarty,<sup>3</sup> S. Strauch,<sup>10</sup> A. Adeyemi,<sup>1</sup> K. Allada,<sup>11</sup> W. Armstrong,<sup>12</sup> J. Arrington,<sup>13</sup> H. Arenhövel,<sup>14</sup> A. Beck,<sup>15</sup> F. Benmokhtar,<sup>16</sup> B. L. Berman,<sup>17</sup> W. Boeglin,<sup>18</sup> E. Brash,<sup>19</sup> A. Camsonne,<sup>8</sup> J. Calarco,<sup>20</sup> J. P. Chen,<sup>8</sup> S. Choi,<sup>6</sup> E. Chudakov,<sup>8</sup> L. Coman,<sup>21</sup> B. Craver,<sup>21</sup> F. Cusanno,<sup>22</sup> J. Dumas,<sup>7</sup> C. Dutta,<sup>11</sup> R. Feuerbach,<sup>8</sup> A. Freyberger,<sup>8</sup> S. Frullani,<sup>22</sup> F. Garibaldi,<sup>22</sup> J.-O. Hansen,<sup>8</sup> T. Holmstrom,<sup>23</sup> C. E. Hyde,<sup>24,25</sup> H. Ibrahim,<sup>26</sup> Y. Ilieva,<sup>17</sup> X. Jiang,<sup>7</sup> M. K. Jones,<sup>8</sup> A. T. Katramatou,<sup>2</sup> A. Kelleher,<sup>27</sup> E. Khrosinkova,<sup>2</sup> E. Kuchina,<sup>7</sup> G. Kumbartzki,<sup>7</sup> J. J. LeRose,<sup>8</sup> R. Lindgren,<sup>21</sup> P. Markowitz,<sup>18</sup> S. May-Tal Beck,<sup>15</sup> E. McCullough,<sup>3,28</sup> D. Meekins,<sup>8</sup> M. Meziane,<sup>27</sup> Z.-E. Meziani,<sup>12</sup> R. Michaels,<sup>8</sup> B. Moffit,<sup>27</sup> B. E. Norum,<sup>21</sup> G. G. Petratos,<sup>2</sup> Y. Oh,<sup>6</sup> M. Olson,<sup>29</sup> M. Paolone,<sup>10</sup> K. Paschke,<sup>21</sup> C. F. Perdrisat,<sup>27</sup> M. Potokar,<sup>30</sup> R. Pomatsalyuk,<sup>8,31</sup> I. Pomerantz,<sup>9</sup> A. Puckett,<sup>32</sup> V. Punjabi,<sup>33</sup> X. Qian,<sup>34</sup> Y. Qiang,<sup>32</sup> R. D. Ransome,<sup>7</sup> M. Reyhan,<sup>7</sup> J. Roche,<sup>35</sup> Y. Rousseau,<sup>7</sup> B. Sawatzky,<sup>21,12</sup> E. Schulte,<sup>7</sup> M. Schwamb,<sup>14</sup> M. Shabestari,<sup>21</sup> A. Shahinyan,<sup>36</sup> R. Shneur,<sup>9</sup> S. Širca,<sup>37</sup> K. Slifer,<sup>21</sup> P. Solvignon,<sup>13</sup> J. Song,<sup>6</sup> R. Sparks,<sup>8</sup> R. Subedi,<sup>2</sup> G. M. Urciuoli,<sup>22</sup> K. Wang,<sup>21</sup> B. Wojtsekhowski,<sup>8</sup> X. Yan,<sup>6</sup> H. Yao,<sup>12</sup> X. Zhan,<sup>32</sup> and X. Zhu<sup>13,34</sup>

(The Jefferson Lab Hall A Collaboration)

<sup>1</sup>Hampton University, Hampton, VA 23668 USA

<sup>2</sup>Kent State University, Kent, Ohio 44242, USA

<sup>3</sup>Saint Mary's University, Halifax, Nova Scotia B3H 3C3, Canada

<sup>4</sup>Dalhousie University, Halifax, Nova Scotia B3H 3J5, Canada

<sup>5</sup>Weizmann Institute of Science, Rehovot 76100, Israel.

<sup>6</sup>Seoul National University, Seoul 151-747, Korea

<sup>7</sup>Rutgers, The State University of New Jersey, Piscataway, New Jersey 08855, USA

<sup>8</sup>Thomas Jefferson National Accelerator Facility, Newport News, Virginia 23606, USA

<sup>9</sup>Tel Aviv University, Tel Aviv 69978, Israel

<sup>10</sup>University of South Carolina, Columbia, South Carolina 29208, USA

<sup>11</sup>University of Kentucky, Lexington, Kentucky 40506, USA

<sup>12</sup>Temple University, Philadelphia, Pennsylvania 19122, USA

<sup>13</sup>Argonne National Laboratory, Argonne, Illinois 60439, USA

<sup>14</sup>Institut für Kernphysik, Johannes Gutenberg-Universität, D-55099 Mainz, Germany

<sup>15</sup>NRCN, P.O. Box 9001, Beer-Sheva 84190, Israel

<sup>16</sup>Duquesne University, Pittsburgh, PA 15282 USA

<sup>17</sup>George Washington University, Washington, D.C. 20052, USA

<sup>18</sup>Florida International University, Miami, Florida 33199, USA

<sup>19</sup>Christopher Newport University, Newport News, Virginia 23606, USA

<sup>20</sup>University of New Hampshire, Durham, New Hampshire 03824, USA

<sup>21</sup>University of Virginia, Charlottesville, Virginia 22094, USA

<sup>22</sup>INFN, Sezione Sanità and Istituto Superiore di Sanità, Laboratorio di Fisica, I-00161 Rome, Italy

<sup>23</sup>Longwood University, Farmville, Virginia, 23909, USA

<sup>24</sup>Old Dominion University, Norfolk, Virginia 23508, USA

<sup>25</sup>Université Blaise Pascal / CNRS-IN2P3, F-63177 Aubière, France

<sup>26</sup>24 Cairo University, Giza 12613, Egypt

<sup>27</sup>College of William and Mary, Williamsburg, Virginia 23187, USA

<sup>28</sup>University of Western Ontario, London, Ontario N6A 3K7, Canada.

<sup>29</sup>Saint Norbert College, Greenbay, Wisconsin 54115, USA

<sup>30</sup>Jožef Stefan Institute, 1000 Ljubljana, Slovenia

<sup>31</sup>NSC Kharkov Institute of Physics and Technology, Kharkov 61108, Ukraine

<sup>32</sup>Massachusetts Institute of Technology, Cambridge, Massachusetts 02139, USA

<sup>33</sup>Norfolk State University, Norfolk, Virginia 23504, USA

<sup>34</sup>Duke University, Durham, North Carolina 27708, USA

<sup>35</sup>Ohio University, Athens, Ohio 45701, USA

<sup>36</sup>Yerevan Physics Institute, Yerevan 375036, Armenia

<sup>37</sup>Dept. of Physics, University of Ljubljana, 1000 Ljubljana, Slovenia

(Dated: December 14, 2024)

**Background:** Two-photon exchange contributions have become a necessary ingredient in theoretical calculations trying to precisely calculate hydrogen elastic scattering cross sections. This correction typically modifies the cross section at the few percent level. In contrast, dispersive effects can cause significantly larger changes from the Born approximation.

**Purpose:** The purpose of this experiment is to measure the carbon-12 elastic cross section around the first diffractive minimum, where the Born term contributions to the cross section are small to maximize the sensitivity to dispersive effects.

**Methods:** This experiment used the high resolution Jefferson Lab Hall A spectrometers to measure the cross sections near the first diffraction minimum of  $^{12}\text{C}$  at beam energies of 362 MeV and 685 MeV.

**Results:** The results are in very good agreement with previous world data. The average deviation from a static charge distribution expected from linear and quadratic fits indicate a 38.8% contribution of dispersive effects to the cross section at 1 GeV.

**Conclusions:** The magnitude of the dispersive effects near the first diffraction minimum of  $^{12}\text{C}$  has been confirmed to be large with a strong energy dependence and could account for a large fraction of the magnitude for the observed quenching of the longitudinal nuclear response. These effects could also be important for nucleon radii extracted from parity violating asymmetries measured near a diffractive minimum.

## I. INTRODUCTION

During the 80s and 90s, higher order corrections to the first Born approximation were extensively studied through dedicated elastic and quasi-elastic scattering experiments using unpolarized electron and positron beams (see [1–6] and references therein). These effects scale as  $S_{HOB} = V_C/E_{inc}$  where  $S_{HOB}$  is the scaling factor to account for higher order corrections to the Born approximation,  $V_C$  is the Coulomb potential of the target nucleus and  $E_{inc}$  is the incident energy of the lepton probe. Therefore, they have been neglected in the analysis of GeV energy data:  $V_C$  reaches a maximum of about 26 MeV for  $^{208}\text{Pb}$  with a corresponding value of  $S_{HOB} = 0.52\%$  for a 5 GeV beam.

In the 1<sup>st</sup> order approximation, the scattering cross section is evaluated using plane wave functions for the incoming and outgoing electrons. This approach is also known as the Plane Wave Born approximation (PWBA) or simply the Born Approximation (Fig. 1). Coulomb corrections originate from the Coulomb field of the target nucleus that causes an acceleration (deceleration) of the incoming (outgoing) electrons and a Coulomb distortion of the plane wave: these effects are treated within a Distorted Wave Born Approximation (DWBA) analysis for inelastic scattering or elastic/quasi-elastic scattering on heavy nuclei [6]. Two other corrections are required to properly evaluate the scattering cross section: radiative corrections due to energy loss processes and dispersive effects due to virtual excitations of the nucleus at the moment of the interaction (Fig. 1).

Within the last decade, a renewed interest arose from a discrepancy between unpolarized and polarized elastic scattering data on the measurement of the proton form factor ratio  $\mu G_E^p/G_M^p$  which can be attributed to the contribution of two-photon exchanges [7–14]. These effects have been investigated with a series of dedicated experiments [15–18] (also see reviews [19–21] and references therein), including their impact on the measurement of form factors for nucleons and light ( $A \leq 3$ ) nuclei. They include both Coulomb corrections [6, 22] and treatment of the off-shell nucleons through dispersion relations as a function of the 4-momentum transfer.

Coulomb corrections have historically been labeled as

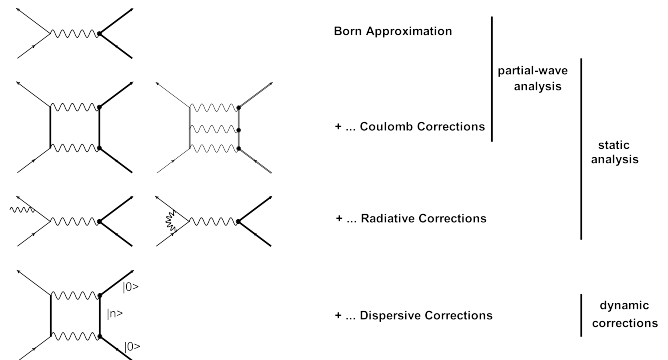


FIG. 1. High-order corrections to the one-photon exchange Born approximation in electron/positron-nucleus scattering.

*static* corrections to the Born approximation as depicted in Fig. 1. While these effects contribute to a few percents [6, 19, 20, 22], *dynamic* corrections known as dispersive effects are energy dependent and are emphasized in the diffraction minima, where the first-order (Born approximation) cross section has a zero: they can contribute up to 18% to the Born approximation in the first diffraction minimum of  $^{12}\text{C}$  at 690 MeV [4, 5].

The electromagnetic nuclear elastic cross section for electrons can be expressed as:

$$\frac{d\sigma}{d\Omega} = \left( \frac{d\sigma}{d\Omega} \right)_{Mott} |F(q)|^2 \quad (1)$$

where  $\left( \frac{d\sigma}{d\Omega} \right)_{Mott}$  is the Mott cross section corresponding to the scattering on a point-like nuclear target,  $F(q)$  represents the form factor and  $q = -Q^2$  is the 4-momentum transfer.

Theoretical calculations for dispersive effects in elastic electron scattering on  $^{12}\text{C}$  were performed in the mid-70s by Friar and Rosen [23]. They used a harmonic oscillator model and only the longitudinal (Coulomb) component to calculate the scattering amplitude within the DWBA approximation; the transverse component was neglected. The matrix element in the center-of-mass frame – considering only the contribution from the dominant two

photon exchange diagrams – can be written as:

$$\mathcal{M}_{disp} = \sum_{n \neq 0} \int \frac{d^3\vec{p}}{\vec{q}_1 \vec{q}_2} \frac{\langle 0 | \rho(\vec{q}_2) | n \rangle \langle n | \rho(\vec{q}_1) | 0 \rangle}{p^2 - p_n^2 - i\varepsilon} a(p_n) \quad (2)$$

with:

$$\begin{cases} a(p_n) &= E_e p_n [1 + \cos \theta] + \vec{p} \cdot (\vec{p}_e + \vec{p}_{e'}) \\ p_n &= E_e - \omega_n - \frac{p^2 - E_e^2}{2M_p} \\ p &= p_e - p_{e'} \end{cases} \quad (3)$$

where:  $p_e = (E_e, \vec{p}_e)$  and  $p_{e'} = (E_{e'}, \vec{p}_{e'})$  the 4-momentum of the incoming and outgoing electrons, respectively, and  $\vec{q}_{1,2}$  the 3-momenta of the two photons exchanged.  $\theta$  is the angle between the incoming and outgoing electrons. In their calculation, Friar and Rosen [23] considered that all nuclear excitation states  $|n\rangle$  have the same mean excitation energy  $\omega$ , allowing to apply the closure relation:  $\sum |n\rangle \langle n| = 1$ .  $\mathcal{M}_{disp}$  can be re-written in a more simplistic form:

$$\mathcal{M}_{disp} = (\alpha Z)F(q) + (\alpha Z)^2 G(q) \quad (4)$$

with  $G(q)$  arising from two-photon exchange diagrams (including cross-diagram, seagull ...) leading to:

$$\begin{aligned} |\mathcal{M}_{disp}|^2 &= (\alpha Z)^2 [F(q)]^2 + 2(\alpha Z)^3 [F(q)\mathcal{R}e\{G(q)\}] \\ &+ (\alpha Z)^4 [|\mathcal{R}e\{G(q)\}|^2 + |\mathcal{I}m\{G(q)\}|^2] \end{aligned} \quad (5)$$

Therefore, the scattering amplitude is governed by  $F(q)$  and the real part of  $G(q)$  outside the minima of diffraction (where  $F(q) \neq 0$ ). The imaginary part of  $G(q)$  contributes in the minima of diffraction where  $F(q_{min}) = 0$ .

Experimentally, in order to extract the magnitude of the dispersive effects, the momentum transfer  $q$  is modified to account for the Coulomb effects into an effective momentum transfer  $q_{eff}$ . The latter is obtained by modifying the incident ( $E = E_e$ ) and scattered ( $E' = E_{e'}$ ) energies of the incoming and outgoing electrons [6]:

$$q = 4EE' \sin^2(\Theta/2) \rightarrow q_{eff} = 4E_{eff}E'_{eff} \sin^2(\theta/2) \quad (6)$$

with  $E_{eff} = E \left(1 - \frac{|V_C|}{E}\right)$  and  $E'_{eff} = E' \left(1 - \frac{|V_C|}{E'}\right)$ .  $|V_C|$  is the (magnitude of the) Coulomb potential of the target nucleus.

The corresponding experimentally measured cross section can then be compared to the theoretical cross section calculated using a static charge density [4]. This paper reports on a recent analysis of these effects in the first diffraction minimum of  $^{12}\text{C}$  at  $q_{eff} = 1.84 \text{ fm}^{-1}$  performed in the experimental Hall A at Jefferson Lab [24, 25].

## II. THE LEDEX EXPERIMENTAL SETUP

The Low Energy Deuteron EXperiment (LEDEX) [24] was performed in two phases: first in late 2006 with a

beam energy of 685 MeV and then in early 2007 with a beam energy of 362 MeV. They both used a 99.95 % pure  $^{12}\text{C}$  target with a density of  $2.26 \text{ g/cm}^3$  and a thickness of  $0.083 \pm 0.001 \text{ g/cm}^2$ . The combined momentum transfer range was  $0.4 - 3.0 \text{ fm}^{-1}$ .

The two identical high-resolution spectrometers (HRS) [26] in Hall A were designed for nuclear-structure studies through the  $(e, e'p)$  reaction. Each contains three quadrupoles and a dipole magnet, all superconducting and cryogenically cooled, arranged in a QQDQ configuration. While the first quadrupoles focus the scattered particles, the dipole steers the charged particles in a  $45^\circ$  upward angle, and the last quadrupole allows one to achieve the desired horizontal position and angular resolution. The HRS detector systems are located behind the latter to detect scattered electrons or electro-produced/recoiled hadrons. Each contains a pair of vertical drift chambers for tracking purpose [27], a set of scintillator plans, a Čerenkov detector [28] and a two layer calorimeter for particle identification. During the LEDEX experiment, both spectrometers were tuned to detect elastically scattered electrons. The electrons which do not interact with the target are transported in a beam pipe and eventually stopped in a beam dump located about 20 m downstream of the target.

The position of the left HRS (with respect to the incident beam direction) was changed according to the kinematic settings while the right HRS was fixed at  $24^\circ$  for calibration purposes. The study of the optics for each of the HRS spectrometers was performed with tungsten sieve plates that were mounted in front of each spectrometer. These plates each have a 7 by 7 pattern of 49 holes. Two holes have a diameter of 4 mm while the remaining holes have a 2 mm diameter. The larger holes are placed asymmetrically so that their orientation in the image at the focal plan can be identified without any ambiguity. Further details on this experimental setup can be found in [29].

For the elastic measurements, a 2 msr tungsten collimator was mounted to the face of the spectrometers: it has a  $3 \times 6 \text{ cm}^2$  rectangular hole at its center, nineteen 2 mm diameter pin holes symmetrically placed around it and one 4 mm diameter pin hole in the bottom corner of the central large opening as shown in Fig. 2. The physical locations of these holes were surveyed before the start of the experiment. This redundant calibration check is performed to eliminate any ambiguity in the scattering angle (Fig. 3): the 2D distribution of the spectrometer angles  $\phi = \phi_{spec}$  (horizontal) and  $\theta = \theta_{spec}$  (vertical) shows an asymmetric trapezoid reflecting the dependence of the cross section when going horizontally from  $-0.03 \text{ mrad}$  (lower scattering angle) to  $0.03 \text{ mrad}$  (larger scattering angle).

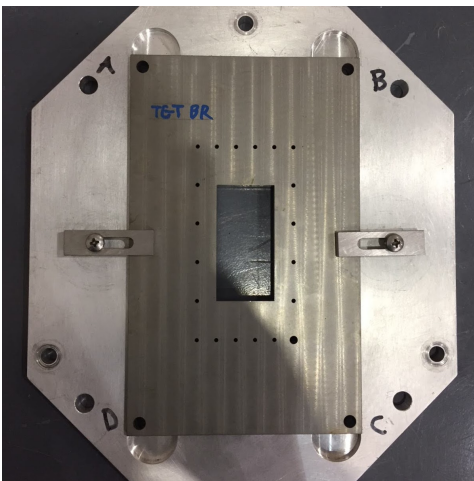


FIG. 2. Photo of the tungsten (grey) 2 mrs collimator with its outer sieve holes that was used during this experiment. The outer aluminum frame mounted to the face of the HRS spectrometer with mounting bolts located at A,B,C and D. The tungsten plate could be removed if full HRS acceptance was desired without removing the outer aluminum frame. Sieve photo courtesy of Jessie Butler.

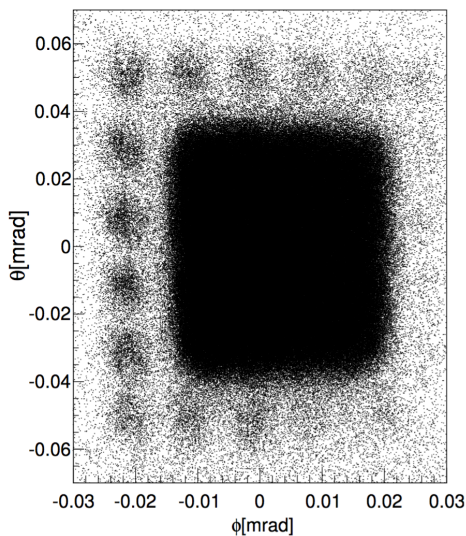


FIG. 3. The experimentally reconstructed scattering ( $\phi$ ) and azimuthal ( $\theta$ ) spectrometer angles with the tungsten collimator installed. The 2 mrs opening is clearly visible. Due to the rapid decrease in the elastic cross section, only the small scattering angle sieve holes are visible.

### III. DATA ANALYSIS

The differential elastic scattering cross-sections were measured using Eq. (7):

$$\frac{d\sigma}{d\Omega} = \frac{P_S \times N_{net}}{L \times t \times \Delta\Omega \times \prod_i \epsilon_i} \times R \quad (7)$$

where:  $P_S$  is the pre-scale factor,  $N_{net}$  is the net counts (found by subtracting the dummy and background runs

from calibrated runs and after applying necessary acceptance and particle identification cuts),  $L$  is the luminosity of the run,  $t$  is the duration of the run,  $\Delta\Omega$  is the solid angle,  $\prod_i \epsilon_i$  is the running (electronics, computer and cuts) efficiencies and  $R$  is the radiative corrections factor. The luminosity for fixed target is calculated from  $L = \mathcal{F}_e d_T l$ , with  $\mathcal{F}_e$  the incident particle flux or number of incoming particles per second,  $d_T$  the density of the target, and  $l$  the target thickness.

The radiative corrections factor,  $R$ , cannot be evaluated experimentally: the MCEEP-Monte Carlo simulation code for  $(e, e'p)$  [30] was used for that purpose. In MCEEP, the virtual photons are taken into account through a Schwinger term [31], found by the Penner calculation. The elastic radiative tail due to hard photons is approximated from the prescription by Mo and Tsai [32]. MCEEP also accounts for the external radiation sources such as straggling, external Bremsstrahlung, energy losses from multiple collisions with the atomic electrons etc. This simulation package was also used to calculate the phase space factors [30]. Dead times (both electronic and computer) were found to be negligible for this experiment, and the tracking and triggering efficiencies found to be more than 99%.

The maximum beam current achieved was  $19.5 \mu A$  at 362 MeV and  $23.4 \mu A$  at 685 MeV. Table I lists the primary sources of systematic uncertainties for the LEDEX experiment. Note listed is the uncertainty on the incident beam position of  $\pm 200 \mu m$ . Around the diffraction minima, the statistical uncertainty dominates translating to: 7.70% (statistical) and 3.50% (systematic) at 362 MeV and 4.24% (statistical) and 2.40% (systematic) at 685 MeV. The situation is exactly the opposite outside the diffraction minima [25].

TABLE I. Systematic Uncertainties for the LEDEX experiment [25].

Quantity	Normalization	
	Random [%]	Systematic [%]
Beam Energy	0.03	—
Beam Current	0.50	—
Solid Angle	1.00	—
Target Composition	0.05	—
Target thickness	0.60	—
Tracking Efficiency	—	1.00
Radiation correction	1.00	—
Background Subtraction	—	1.00

Figs. 4 and 5 show the reconstructed excitation energy distributions at 362 MeV and 685 MeV incident beam energies, respectively. The high resolution of the HRS spectrometers (0.05%) allows to clearly identify the first three excited states of  $^{12}C$  for both energies: 4.44 MeV ( $2^+$ ), 7.65 MeV ( $0^+$ ) and 9.64 MeV ( $3^-$ ). This paper reports on the analysis of the elastic peak data.

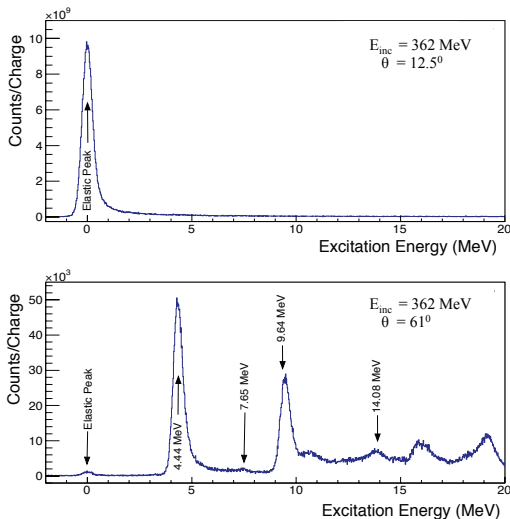


FIG. 4. The reconstructed excitation energy distributions at  $E_{inc} = 362$  MeV for  $\theta = 12.5^\circ$  (top) and  $\theta = 61^\circ$  (bottom) scattering angles.

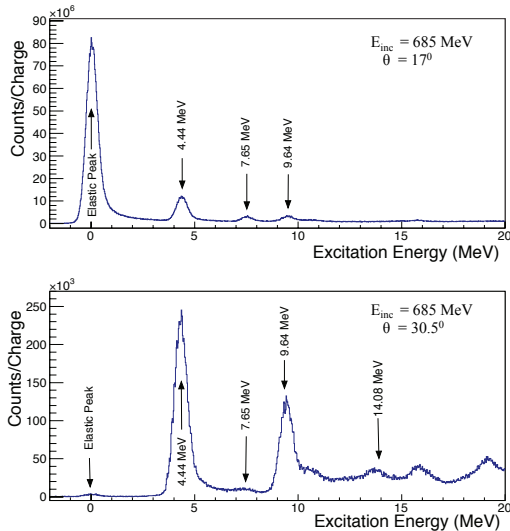


FIG. 5. The reconstructed excitation energy distributions at  $E_{inc} = 685$  MeV for  $\theta = 17^\circ$  (top) and  $\theta = 30.5^\circ$  (bottom) scattering angles.

#### IV. RESULTS

The measured elastic cross sections inside the first diffraction minimum of  $^{12}\text{C}$  were found to be  $4.56 \pm 0.39$  mb for (362 MeV,  $61^\circ$ ) and  $19.96 \pm 0.97$  mb for (685 MeV,  $30.5^\circ$ ) corresponding to 4-momentum transfers (see Table II)  $q$  of  $1.85 \text{ fm}^{-1}$  and  $1.82 \text{ fm}^{-1}$  ( $q_{eff}$  of  $1.82 \text{ fm}^{-1}$  and  $1.81 \text{ fm}^{-1}$ ), respectively. They were compared to

the cross sections calculated using a static charge distribution. A Fourier-Bessel (F-B) parameterization was used identical to the one from Offermann *et al.* [4].

TABLE II. The four-momentum transfer ( $q$ ) and effective 4-momentum transfer ( $q_{eff}$ ) for the LEDEX experiment for each elastic kinematic setting calculated using Eq. (6).

$E$ (MeV)	$\theta$ (Deg.)	$E'$ (MeV)	$q$ ( $\text{fm}^{-1}$ )	$q_{eff}$ ( $\text{fm}^{-1}$ )
362	12.5	361.722	0.399	0.394
362	61.0	356.056	1.847	1.821
685	17.0	683.170	1.025	1.017
685	30.5	679.237	1.819	1.805

The results of this analysis was also compared to the world data (see Fig. 6). A first order (solid line) and second order (dashed line) polynomial fits (see Table III) predict deviations at 1 GeV of 30.69% and 46.93%, respectively (average of 38.81%).

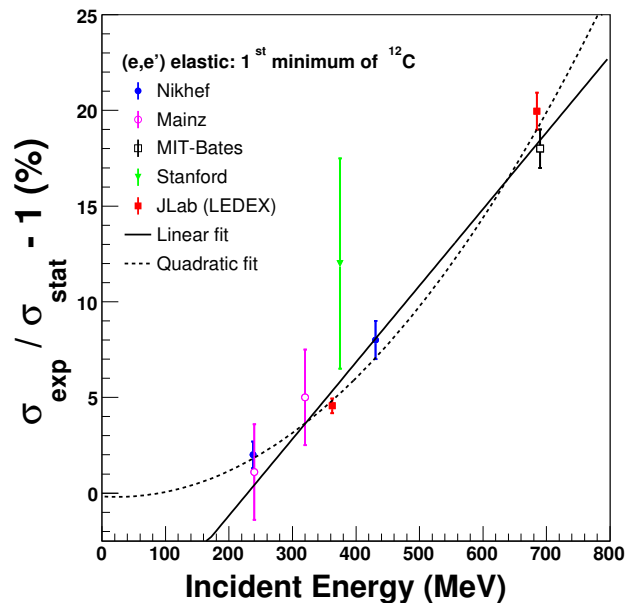


FIG. 6. World data on the energy dependence of dispersive effects in the first diffraction minimum of  $^{12}\text{C}$ . The first minimum at  $q_{eff} = 1.84 \text{ fm}^{-1}$  moves slightly with beam energy as noted in [33] (this dependency is out of the scope of this paper).

The theoretical prediction from Friar and Rosen [23] on the size of dispersive effects in the first diffraction minimum of  $^{12}\text{C}$  is shown in Fig. 7 for 374.5 MeV and 747.2 MeV where the inclusion of dispersive corrections  $\sigma_{stat+disp}$  is compared to the cross section  $\sigma_{stat}$  obtained from a static charge distribution: the expected (constant) 2% predicted discrepancy is clearly not reproducing the magnitude and energy dependence behavior seen in the data.

TABLE III. Polynomial fit parameters on the world data set for dispersive effects in the first minimum of  $^{12}\text{C}$ .

	Linear Fit	Quadratic Fit
$p_0$	$-9.307 \pm 0.851$	$-0.070 \pm 3.173$
$p_1(10^{-2} \text{ MeV}^{-1})$	$+4.026 \pm 0.201$	$-0.274 \pm 1.438$
$p_2(10^{-5} \text{ MeV}^{-2})$		$+4.450 \pm 1.473$
$\chi^2/ndf$	15.202/6	6.072/5

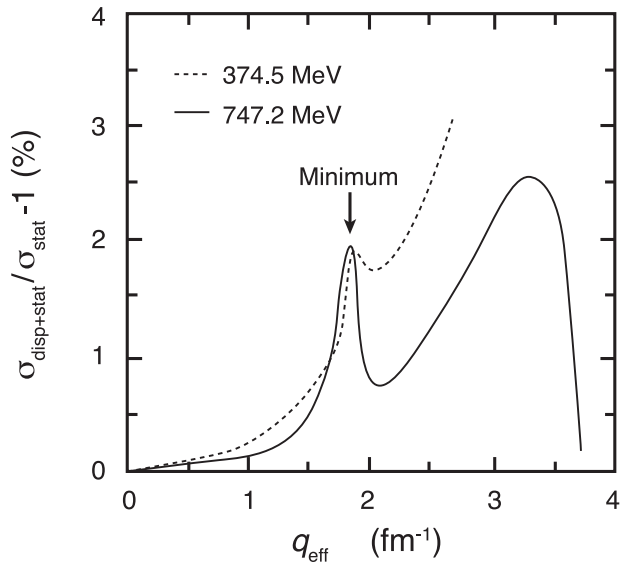


FIG. 7. Calculations of Friar and Rosen [23] for dispersion corrections to elastic electron scattering from  $^{12}\text{C}$  at 374.5 and 747.2 MeV in the first diffraction minimum  $q_{eff} = 1.84 \text{ fm}^{-1}$ .

## V. DISPERSIVE CORRECTIONS AND THE NUCLEAR MATTER

A very simplistic approach is now used to estimate the effects of dispersive corrections with our linear and quadratic fits on two specific observables: the nuclear charge density [34, 35] and the Coulomb Sum Rule [36].

Coulomb corrections stem from multi-photons exchange between the incoming lepton probe and the target nucleus, with  $2\gamma$  being the dominant contribution due to the low electromagnetic coupling constant  $\alpha = 1/137$ . To accurately estimate these effects, one should take into account the continuous change of the incident beam energy while the particle is approaching the nucleus. In practice, one assumes a constant Coulomb field to estimate these effects and applies an effective global shift of the incident and outgoing beam energies as described in Section I. Note that one should use the average Coulomb potential  $|V_C| = \int \rho(r)|V_C|(r)d^3r/Z|e|$  instead of the potential at the origin of the nucleus  $|V_C(0)|$  [6].

The dispersive cross section  $\sigma_{disp} = \sigma_{stat+disp}$  (for simplicity) can be expressed as a function of the cross section  $\sigma_{stat}$  as:

$$\sigma_{disp} = \sigma_{stat}[1 + \delta(E_{inc})] \quad (8)$$

with  $\delta(E_{inc})$  the higher order correction contribution to the Born Approximation. Coulomb corrections can thus be understood as the zero'th order correction of the energy dependence arising from dispersion corrections (taking radiative corrections into account as depicted in Fig. 1) :

$$\sigma_{stat} = \sigma_{Born}[1 + \delta(0)] \quad (9)$$

### A. Effects on nuclear radii

The form factor  $F(q)$  in equation (1) can be re-written in terms of  $F_{p,n}(q)$  with

$$F_{p,n}(q) = \frac{1}{4\pi} \int d^3r j_0(qr) \rho_{p,n}(r) \quad (10)$$

the charge form factor of the proton (p) or neutron (n) and  $j_0(r) = \sin(qr)/qr$  the zero'th spherical Bessel function. The proton ( $R_p$ ) and neutron ( $R_n$ ) radii can be determined from (experimentally measured)  $F_{p,n}$  as:

$$ZF_p = 4\pi \int_0^\infty \rho_p r^2 dr = \sum_{\nu=1}^\infty (-1)^{\nu+1} \frac{4\pi R_p}{q_\nu^2} a_\nu \quad (11)$$

$$NF_n = 4\pi \int_0^\infty \rho_n r^2 dr = \sum_{\nu=1}^\infty (-1)^{\nu+1} \frac{4\pi R_n}{q_\nu^2} b_\nu \quad (12)$$

A similar expression for the weak charge radius  $R_w$  of a nucleus can be extracted from parity-violating experiments [34, 35].

Plugging Eq. 9 in Eqs. 1, 10, and using Eqs. 11-12 leads to:

$$R_{p,n}^{disp} = R_{p,n}^{stat} \times [1 + \delta(E_{inc})] \quad (13)$$

The Coulomb field extracted from  $R_p$  should then also be modified from

$$|V_C| = |V_C^{stat}| = \frac{KZ}{\langle r^2 \rangle^{1/2}} ; K = 1/4\pi\epsilon_0 \quad (14)$$

to

$$|V_C^{disp}| = |V_C^{stat}| / [1 + \delta(E_{inc})] \quad (15)$$

Equation 15 implies a subsequent change in the nuclear charge density  $\rho$ :

$$\rho^{disp} = \rho^{stat} / [1 + \delta(E_{inc})] \quad (16)$$

As mentioned previously, Coulomb corrections are expected to be comparatively small for GeV energies:  $S_{HOB} = 2.6\%$  for a 1 GeV incident electron beam on a  $^{208}\text{Pb}$  target. In the remainder of this section, we will assume that the energy dependent correction is solely rising from dispersive corrections and is embedded in the term  $\delta(E_{inc})$ .

In our naive model, one can assume that a change of the measured (charge) form factor translates in a change of the nucleon size. Using the fits parameters from Table III, these corrections are expected to be around 39% at 1 GeV for  $^{12}\text{C}$ . A detailed analysis of their impact on nuclear radii was performed by Offerman et al. [4]: the result is a net relatively small effect of 0.28%, implying a renormalization of the charge distribution to offset the change in the cross section.

In order to estimate the corrections for  $^{208}\text{Pb}$ , we scale the carbon value using Coulomb fields from [6]:

$$0.28\% \frac{V_{C,208\text{Pb}} = 18.5 \text{ MeV}}{V_{C,12\text{C}} = 5.0 \text{ MeV}} \frac{Z_{12\text{C}} = 6}{Z_{208\text{Pb}} = 82} = 0.08\%. \quad (17)$$

Note that a similar scaling of the 39% predicted corrections on  $^{12}\text{C}$  translates to an 11% on  $^{208}\text{Pb}$  which is compatible with the  $\sim 6\%$  effect observed by Breton *et al.* [3]. The value of about 0.08% should be taken as the correction from dispersive effects on  $R_p$  for lead. It is reasonable to assume that elastic ( $e, n$ ) scattering will undergo similar higher order corrections as elastic ( $e, p$ ) scattering within the nuclear matter.

The situation is far more complex for parity violating experiments [34, 35, 37]. It is clear one should take dispersive effects into account; however, to our knowledge, there is no known measurements of dispersive effects using polarized beams and/or target. Therefore, measurements of the energy dependence for dispersive effects using polarized elastic scattering on various nuclear targets ( $A > 1$ ) should be performed to provide an accurate information about the size of these effects in and outside minima of diffraction.

### B. Effects on the Coulomb Sum Rule

The Coulomb Sum Rule (CSR) [38] is defined as the integral of the longitudinal response function  $R_L(\omega, |\mathbf{q}|)$  extracted from quasi-elastic electron scattering:

$$S_L(|\mathbf{q}|) = \int_{\omega>0}^{|\mathbf{q}|} \frac{R_L(\omega, |\mathbf{q}|)}{ZG_{E_p}^2(Q^2) + NG_{E_n}^2(Q^2)} \quad (18)$$

where  $-Q^2 = \omega^2 - \vec{q}^2$  with  $\omega$  the energy transfer and  $\vec{q}$  the three-momentum transfer.  $G_{E_{p,n}}(Q^2)$  is the proton (neutron) form factor which reduces to the Sachs electric form factor if the nucleon is not modified by the nuclear medium [39].  $\omega > 0$  ensures that the integration is performed above the elastic peak.

In quasi-elastic scattering, the quenching of CSR has been found to be as much as 30% [36] for medium and heavy nuclei. Using a quantum field-theoretic quark-level approach which preserves the symmetries of quantum chromodynamics, as well as exhibiting dynamical chiral symmetry breaking and quark confinement, Cloet *et al.* [40] recently confirmed the dramatic quenching of the Coulomb Sum Rule for momentum transfers  $|q| \gtrsim 0.5 \text{ GeV}$

that lies in changes to the proton Dirac form factor induced by the nuclear medium.

From our naive model:

$$G_{E_{p,n}}^{disp}(Q^2) = \frac{G_{E_{p,n}}^{stat}(Q^2)}{1 + \delta(E_{inc})} \quad (19)$$

Hence:

$$S_L^{disp}(|\mathbf{q}|) = S_L^{stat}(|\mathbf{q}|) \times [1 + \delta(E_{inc})] \quad (20)$$

Using Fig. 6 for a 600 MeV incident beam on  $^{12}\text{C}$ , one would expect a 14% correction in the minimum of diffraction, which is a factor of 7 from the 2% prediction from Friar and Rosen [23]. Above the minimum, their prediction indicates an almost linear increase of the dispersion corrections up to about  $3.3 \text{ fm}^{-1}$  where it reaches a maximum of about 3%. Assuming the same scaling, that is a  $0.03 \times 7 \simeq 21\%$  predicted effect in the kinematic regime of the CSR data for  $^{12}\text{C}$  [41]. Therefore, dispersion corrections could have a significant contribution on the CSR quenching if the experimentally measured longitudinal response function  $R_L(\omega, |\mathbf{q}|)$  is corrected for these effects.

## VI. CONCLUSION

We have presented new results on the energy dependence for *dynamic* dispersion corrections in elastic electron scattering in the first diffraction minimum of  $^{12}\text{C}$  at  $q = 1.84 \text{ fm}^{-1}$  from Jefferson Lab obtained at two different energies: 362 MeV and 685 MeV [24]. The results are in very good agreement with previous world data on this topic and cannot be explained with available theoretical calculations. Using global fits on the world data set, we have investigated the impact of these corrections on the nuclear charge density. While we find this contribution is around 0.08% for the recent measurement of the nucleon radii from Pb [34, 35, 37], and while it will take a detailed investigation and theory to understand how this effects the parity violating asymmetry, it is expected to be much larger on the observed quenching of the Coulomb Sum Rule [40]. Therefore, we conclude it is important that a systematic study of the dispersion corrections inside and outside diffractive minima for a large range of (light through heavy) nuclei be performed using both unpolarized and polarized beams/targets to help provide a more complete understanding of elastic (and inelastic) electron/positron-nucleus scattering.

## ACKNOWLEDGEMENTS

We thank Larry Cardman for many useful discussions. This work was supported by the Department of Energy National Nuclear Security Administration under award number DE-NA0000979, by the U.S. Department of Energy grant DE-AC02-06CH11357, by the National Science Foundation grant NSF-PHY-1505615 and

by the U.S. Department of Energy contract DE-AC05-06OR23177 under which Jefferson Science Associates op-

erates the Thomas Jefferson National Accelerator Facility.

- 
- [1] L. S. Cardman, J. W. Lightbody, S. Penner, S. P. Fivozinsky, X. K. Maruyama, W. P. Trower, and S. E. Williamson, *Phys. Lett.* **91B**, 203 (1980).
- [2] E. A. J. M. Offermann, C. W. De Jaeger, H. De Vries, L. S. Cardman, H. J. Emrich, G. Fricke, H. Miska, and D. Rychel, *Phys. Rev. Lett.* **57**, 1546 (1986).
- [3] V. Breton *et al.*, *Phys. Rev. Lett.* **66**, 572 (1991).
- [4] E. A. J. M. Offermann, L. S. Cardman, C. W. de Jager, H. Miska, C. de Vries, and H. de Vries, *Phys. Rev.* **C44**, 1096 (1991).
- [5] P. Gueye *et al.*, *Phys. Rev.* **C57**, 2107 (1998).
- [6] P. Gueye *et al.*, *Phys. Rev.* **C60**, 044308 (1999).
- [7] P. A. M. Guichon and M. Vanderhaeghen, *Phys. Rev. Lett.* **91**, 142303 (2003), arXiv:hep-ph/0306007 [hep-ph].
- [8] P. G. Blunden, W. Melnitchouk, and J. A. Tjon, *Phys. Rev. Lett.* **91**, 142304 (2003), arXiv:nucl-th/0306076 [nucl-th].
- [9] M. P. Rekalo and E. Tomasi-Gustafsson, *Eur. Phys. J.* **A22**, 119 (2004), arXiv:hep-ph/0402277 [hep-ph].
- [10] Y. C. Chen, A. Afanasev, S. J. Brodsky, C. E. Carlson, and M. Vanderhaeghen, *Phys. Rev. Lett.* **93**, 122301 (2004), arXiv:hep-ph/0403058 [hep-ph].
- [11] A. V. Afanasev and N. P. Merenkov, *Phys. Rev.* **D70**, 073002 (2004), arXiv:hep-ph/0406127 [hep-ph].
- [12] J. Arrington, *Phys. Rev.* **C71**, 015202 (2005), arXiv:hep-ph/0408261 [hep-ph].
- [13] P. G. Blunden, W. Melnitchouk, and J. A. Tjon, *Phys. Rev.* **C72**, 034612 (2005), arXiv:nucl-th/0506039 [nucl-th].
- [14] P. G. Blunden and W. Melnitchouk, *Phys. Rev.* **C95**, 065209 (2017), arXiv:1703.06181 [nucl-th].
- [15] D. Adikaram *et al.* (CLAS), *Phys. Rev. Lett.* **114**, 062003 (2015), arXiv:1411.6908 [nucl-ex].
- [16] I. A. Rachek *et al.*, *Phys. Rev. Lett.* **114**, 062005 (2015), arXiv:1411.7372 [nucl-ex].
- [17] B. S. Henderson *et al.* (OLYMPUS), *Phys. Rev. Lett.* **118**, 092501 (2017), arXiv:1611.04685 [nucl-ex].
- [18] D. Rimal *et al.* (CLAS), *Phys. Rev.* **C95**, 065201 (2017), arXiv:1603.00315 [nucl-ex].
- [19] C. E. Carlson and M. Vanderhaeghen, *Ann. Rev. Nucl. Part. Sci.* **57**, 171 (2007), arXiv:hep-ph/0701272 [HEP-PH].
- [20] J. Arrington, P. G. Blunden, and W. Melnitchouk, *Prog. Part. Nucl. Phys.* **66**, 782 (2011), arXiv:1105.0951 [nucl-th].
- [21] A. Afanasev, P. G. Blunden, D. Hasell, and B. A. Raue, *Prog. Part. Nucl. Phys.* **95**, 245 (2017), arXiv:1703.03874 [nucl-ex].
- [22] A. Aste, C. von Arx, and D. Trautmann, *Eur. Phys. J.* **A26**, 167 (2005), arXiv:nucl-th/0502074 [nucl-th].
- [23] J. L. Friar and M. Rosen, *Annals Phys.* **87**, 289 (1974).
- [24] R. Gilman, D. W. Higinbotham, X. Jiang, A. Sarty, and S. Strauch, “LEDEX: Low Energy Deuteron EXperiments E05-044 and E05-103 at Jefferson Lab,” (2015).
- [25] A. A. Kabir, *Determination of the charge radii of several light nuclei from precision, high-energy electron elastic scattering*, Ph.D. thesis, Kent State University, Kent State, Ohio (2015).
- [26] J. Alcorn *et al.*, *Nucl. Instrum. Meth.* **A522**, 294 (2004).
- [27] K. G. Fissum *et al.*, *Nucl. Instrum. Meth.* **A474**, 108 (2001).
- [28] M. Iodice *et al.*, *Nucl. Instrum. Meth.* **A411**, 223 (1998).
- [29] B. Lee, *New Precision Measurements of Deuteron Structure Function  $A(Q)$  at Low Momentum Transfer*, Ph.D. thesis, Seoul, Nat. U. Technol. (2009).
- [30] P. E. Ulmer, “Monte Carlo for  $e, e'p$  v3.9,” (2006).
- [31] J. Schwinger, *Phys. Rev.* **75**, 898 (1949).
- [32] L. W. Mo and Y.-S. Tsai, *Rev. Mod. Phys.* **41**, 205 (1969).
- [33] N. Kalantar-Nayestanaki, C. W. De Jager, E. A. J. M. Offermann, H. De Vries, L. S. Cardman, H. J. Emrich, F. W. Hersman, H. Miska, and D. Rychel, *Phys. Rev. Lett.* **63**, 2032 (1989).
- [34] C. J. Horowitz *et al.*, *Phys. Rev.* **C85**, 032501 (2012), arXiv:1202.1468 [nucl-ex].
- [35] S. Abrahamyan *et al.*, *Phys. Rev. Lett.* **108**, 112502 (2012), arXiv:1201.2568 [nucl-ex].
- [36] J. Morgenstern and Z. E. Meziani, *Phys. Lett.* **B515**, 269 (2001), arXiv:nucl-ex/0105016 [nucl-ex].
- [37] S. Abrahamyan *et al.* (HAPPEX, PREX), *Phys. Rev. Lett.* **109**, 192501 (2012), arXiv:1208.6164 [nucl-ex].
- [38] K. W. McVoy and L. Van Hove, *Phys. Rev.* **125**, 1034 (1962).
- [39] J. V. Noble, *Phys. Rev. Lett.* **46**, 412 (1981).
- [40] I. C. Cloët, W. Bentz, and A. W. Thomas, *Phys. Rev. Lett.* **116**, 032701 (2016), arXiv:1506.05875 [nucl-th].
- [41] P. Barreau *et al.*, *Nucl. Phys.* **A402**, 515 (1983).